Amino Wagging and Inversion in Methylamines

Masamichi Tsuboi, Akiko Y. Hirakawa, Takamitsu Ino, Tadahiro Sasaki, and Keietsu Tamagake

Citation: The Journal of Chemical Physics **41**, 2721 (1964); doi: 10.1063/1.1726344
View online: http://dx.doi.org/10.1063/1.1726344
View Table of Contents: http://scitation.aip.org/content/aip/journal/jcp/41/9?ver=pdfcov
Published by the AIP Publishing

in the source.[18] It also extends to the I.E. curves of free radicals, although the observable range below dissociative ionization precludes comparison over the energy range used in this work.[19]

It is a striking characteristic of all curves reported here, and with very few exceptions of all others in related studies, that discontinuities for molecular ions and the onsets of related fragment ions often occur at the same electron energy for ion-pairing processes with positive increments of slope. No depletion of molecular ions is expected for such correlated processes, but neither is the observed increase which cannot now be explained. Both processes however, plausibly arise from a common pre-ionizing state in each instance.

Another remarkable effect is an abrupt *increase* in slope of the molecular I.E. curve often observed at the onset of a fragment ion–neutral process. These correlated discontinuities must be partly accidental, but their prevalence[5–7] requires that many are real. They cannot be attributed to vibrational structure. If they are attributed to excitation potentials of the parent ions to unstable states, then an unacceptably large population of metastable parent ions persists and both metastable molecular and fragment ions increase with increasing electron energy. Moreover, if *A.P.*'s of fragment ions are determined by these widely spaced electronic states of molecular ions, then measured heats of formation of fragment ions by impact methods would be even more divergent than they are. It appears to be necessary to conclude that the onset of dissociative ionization is responsible for an increased yield of molecular ion. It can only be suggested that a common pre-ionized state undergoes branching processes and that the fairly abrupt increase in density of vibrational levels near the dissociation limit could facilitate interstate crossing to increase the cross section for ionization. If both ion–neutral and ion-pair derive from pre-ionized states, the similarity of their respective cross-section dependences upon electron energy can be accounted for.

ACKNOWLEDGMENTS

We are indebted to Professor John L. Magee, Dr. Paul Funabashi, and Dr. Kenjii Fueki for helpful discussions.

---

[18] C. E. Melton and W. H. Hamill, J. Chem. Phys. 41, 1469 (1964).

[19] C. E. Melton and W. H. Hamill, "Ionization Potentials of Alkyl Free Radicals," J. Chem. Phys. (to be published).

THE JOURNAL OF CHEMICAL PHYSICS VOLUME 41, NUMBER 9 1 NOVEMBER 1964

Amino Wagging and Inversion in Methylamines

Masamichi Tsuboi, Akiko Y. Hirakawa, Takamitsu Ino, Tadahiro Sasaki, and Keietsu Tamagake
Faculty of Pharmaceutical Sciences, University of Tokyo, Bunkyo-ku, Tokyo, Japan

(Received 30 June 1964)

Fine structures have been observed of the amino-wagging bands at 780 cm^{-1} of $CH_3{}^{14}NH_2$, at 776 cm^{-1} of $CH_3{}^{15}NH_2$, at 625 cm^{-1} of $CH_3{}^{14}ND_2$, and at 689 cm^{-1} of $CH_3{}^{14}NHD$. For each vibration–rotation line an appreciable inversion splitting is observed. There is a marked coupling found between the inversion and the internal rotation; and the amount of the inversion splitting of each absorption line depends greatly upon the internal rotation quantum number $\sigma(=0, +1, \text{or } -1)$ and the over-all rotation quantum number K of the state in question. A hypothetical inversion splitting when the coupling were absent is estimated to be 31.6 cm^{-1} for the first excited state of the amino-wagging vibration of $CH_3{}^{14}NH_2$.

I. INTRODUCTION

In this paper are reported the results of our observation of the fine structures of amino-wagging bands of four isotopic species of methylamine and the results of our analysis of them.

What are subjected to our present study are the 780-cm^{-1} band of $CH_3{}^{14}NH_2$, 776-cm^{-1} band of $CH_3{}^{15}NH_2$, 625-cm^{-1} band of $CH_3{}^{14}ND_2$, and 689-cm^{-1} band of $CH_3{}^{14}NHD$. According to the result of our normal coordinate treatment, the vibration corresponding to each of the first three bands takes place approximately along a symmetry coordinate shown in Fig. 1. Such a vibration is considered to correspond to the symmetric deformation vibration of ammonia, and along this coordinate an appreciable inversion is expected to take place. In the work described here, appreciable inversion doublings were actually observed. It was also proved, however, that an additional factor which makes the spectra complex should be taken into account in the explanation of the observed fine structures. That is an interaction of inversion and internal rotation. This is what was pointed out by Shimoda, Nishikawa, and Itoh[1–3] and also by Lide and Kivelson[4,5] in their analyses of microwave spectra of methylamines, and may be described briefly in the following way: When the NH_2 group turns over from one side to opposite side of the CH_3 group, the staggered

---

[1] K. Shimoda, T. Nishikawa, and T. Itoh, J. Phys. Soc. Japan 9, 974 (1954).

[2] T. Itoh, J. Phys. Soc. Japan 11, 264 (1956).

[3] T. Nishikawa, J. Phys. Soc. Japan 12, 668 (1957).

[4] D. R. Lide, Jr., J. Chem. Phys. 27, 343 (1957).

[5] D. Kivelson and D. R. Lide, Jr., J. Chem. Phys. 27, 353 (1957).

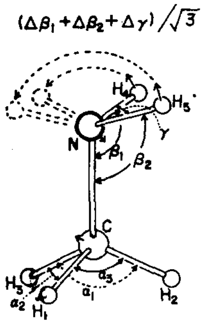

FIG. 1. Molecular structure of methylamine and an approximate expression of the normal coordinate of the amino-wagging vibration.

form becomes the eclipse form—in other words, the minima and maxima of the torsional potential around the C–N bond are reversed. Therefore, after the inversion occurs, an internal rotation should take place to arrive at the minimum position of the potential. This implies a complicated coupling between inversion and internal rotation. Internal rotation, on the other hand, strongly couples with the over-all rotation. Thus, the amount of the inversion splitting Δ depends greatly upon the internal rotation quantum number σ and the rotational quantum number K. An analysis along this line shows that in the methylamine molecule the inversion potential itself is very much similar to that in ammonia. Actually observed inversion doublings, however, are greatly diminished, because of the above mentioned coupling with the internal rotation. For instance, the maximum inversion doubling is only 6.8 cm^{-1} in the first excited state of the wagging vibration in $CH_3{}^{14}NH_2$, in contrast to the corresponding inversion doubling 36.4 cm^{-1} in $^{14}NH_3$.

Brief accounts of some of the results of this investigation have already appeared elsewhere.[6,7]

II. EXPERIMENTAL

Methylamine was obtained from methylamine hydrochloride by adding its concentrated solution to solid sodium hydroxide. Previous purification of the hydrochloride by a recrystallization method was found to be effective for avoiding contamination of ammonia. A commercial sample of methylamine hydrochloride was first dissolved into absolute ethanol. After filtration, the hydrochloride was recrystallized by an addition of ethyl ether. Methylamine gas generated was sent through HgO powder, again in an attempt to remove contaminating ammonia.

Methylamine-^{15}N was prepared from corresponding hydrochloride. The latter was prepared by A. Nakamura from ammonium sulfate in which 98% of nitrogen was ^{15}N and was kindly placed by him at our disposal.

Methylamine-d_2 ($CH_3{}^{14}ND_2$) and methylamine-d ($CH_3{}^{14}NHD$) was prepared by deuterating methylamine by means of a gas chromatograph by a method described by Shimanouchi *et al.*[8] First, D_2O vapor was sent from the exit towards the entrance of a PEG 1000 column heated at 105°–110°C, so that the column was deuterated. Then, methylamine gas was sent from the entrance towards exit as usual, and a deuterated methylamine sample was obtained. When the deuteration was incomplete, the sample contained $CH_3{}^{14}NHD$, and gave the NHD wagging band at 689 cm^{-1} besides the 625-cm^{-1} band of $CH_3{}^{14}ND_2$.

Infrared absorption measurements were made by the use of a Perkin–Elmer Model 112G spectrometer with a 75 line/mm grating blazed at 12 μ and a KBr fore-prism. The practical resolution in the 600–800 cm^{-1} region was found to be slightly better than 1.0 cm^{-1}. In the observation, a gas cell with optical path length of 10 cm was used. The pressure in the gas cell was kept at about 20 mm Hg. The micrometer scale of the wavelength drive of the grating monochromator was checked and corrected in each time of the measurements by observing several absorption lines with known frequencies of H_2O or CO_2.

Figures 2–5 are reproductions of some of the recorded curves.

As may be seen in Fig. 2, the fine structure of the 780 cm^{-1} band of $CH_3{}^{14}NH_2$ is very complicated, and quite different from the fine structures of other bands of $CH_3{}^{14}NH_2$. The fine structures of other bands are rather simple and mostly explained on the basis of the rigid symmetric-top approximation.[9]

The fine structure of the 776-cm^{-1} band of $CH_3{}^{15}NH_2$, given in Fig. 3, is very much similar to that of the 780 cm^{-1} band of $CH_3{}^{14}NH_2$. However, almost every absorption line is found to be shifted by 4.3 cm^{-1} towards lower frequency.

In the absorption band at 625 cm^{-1} of $CH_3{}^{14}ND_2$, there is a series of broad absorption lines located with a spacing of 4.0 cm^{-1}. Almost at midpoint of each spacing, there is a weaker absorption line which is also broad. It was suspected that the series of weaker absorption lines belongs to a hot band superposed on the 625 cm^{-1} band in question. Hence, we examine the temperature effects on the relative intensities of these absorption lines. The absorption cell was heated to 129°C by an electric heating device. The result of this examination is shown in Fig. 6. As may be seen in the figure, the relative intensities of the weaker lines in question (denoted by A, B, and C in the figure) becomes higher as the temperature of the gas is raised.

The fine structure of the 689-cm^{-1} band of $CH_3{}^{14}NHD$ (Fig. 5) is rather simple but it is still anomalous. At the band center there is a twin peaks with a separation

---

[6] M. Tsuboi and A. Y. Hirakawa, VIIth European Congress on Molecular Spectroscopy, A338, Budapest, Hungary, July 1963 (read by T. Shimanouchi).

[7] M. Tsuboi, A. Y. Hirakawa, T. Ino, T. Sasaki, and K. Tamagake, Symposium on Structural Chemistry, 4B18, Sendai, Japan, October 1963.

[8] T. Shimanouchi, C. Tanaka, Y. Toyama, M. Tasumi, and S. Takeda, Kagaku-no-Ryoiki, Zokan 44 (gas chromatography), p. 63, Nanko-do, Tokyo, 1961.

[9] A. P. Grey and R. C. Lord, J. Chem. Phys. **26**, 690 (1957).

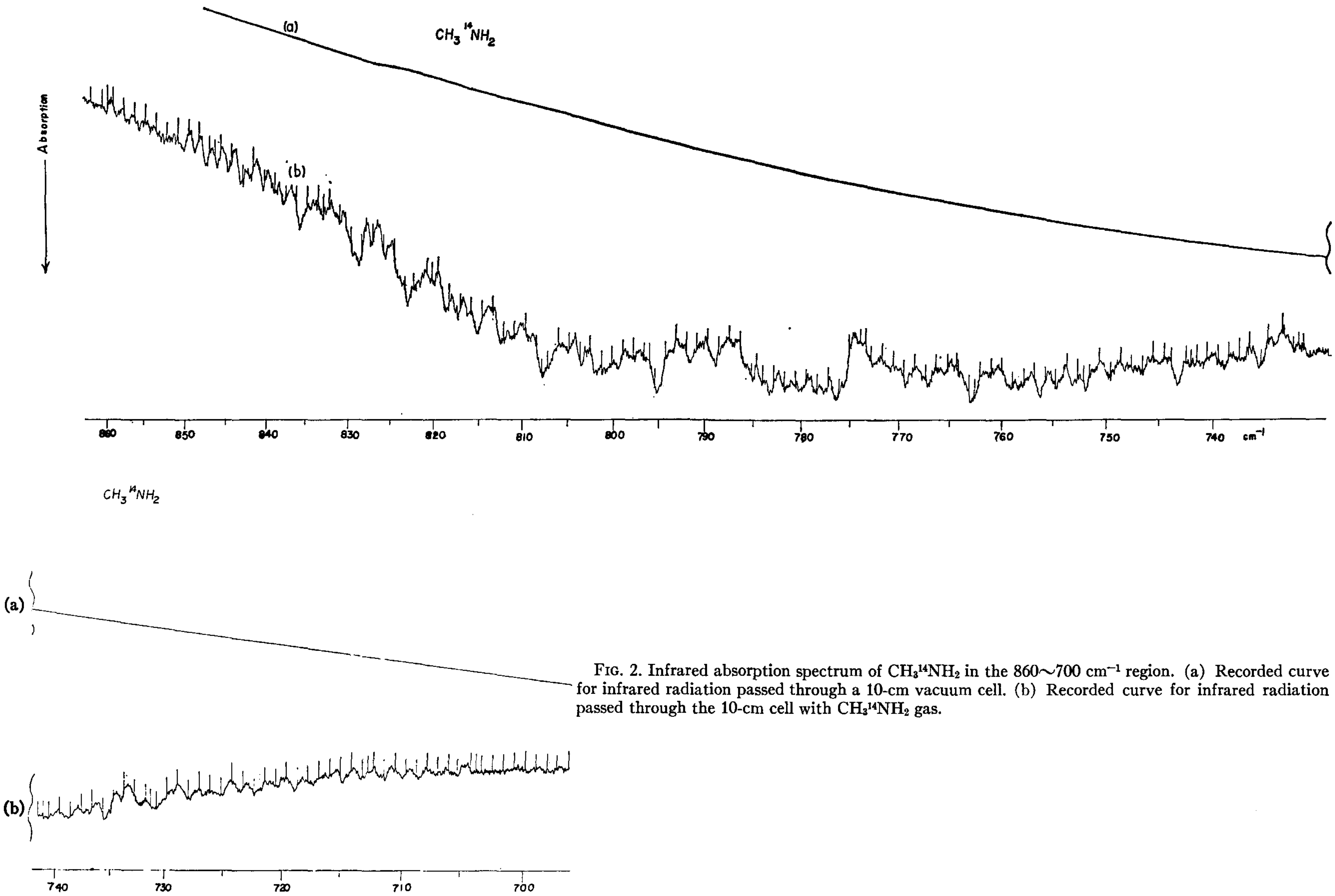

FIG. 2. Infrared absorption spectrum of $CH_3{}^{14}NH_2$ in the 860∼700 cm⁻¹ region. (a) Recorded curve for infrared radiation passed through a 10-cm vacuum cell. (b) Recorded curve for infrared radiation passed through the 10-cm cell with $CH_3{}^{14}NH_2$ gas.

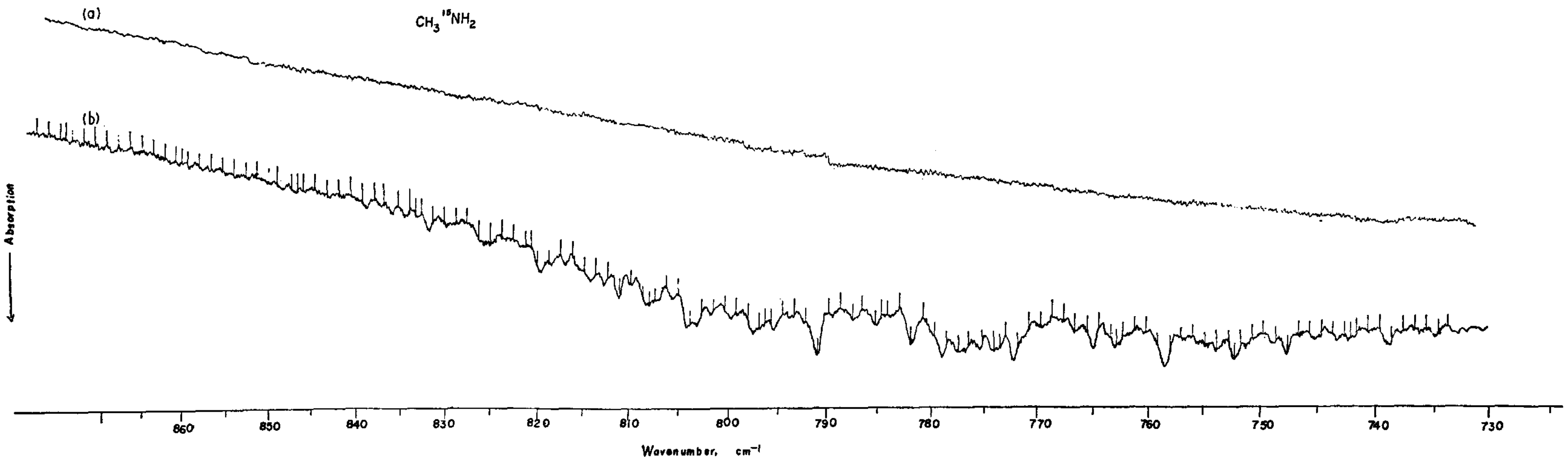

FIG. 3. Infrared absorption spectrum of $CH_3{}^{15}NH_2$ in the 860∼730 cm^{-1} region. (a) Recorded curve for infrared radiation passed through a 10-cm vacuum cell. (b) Recorded curve for infrared radiation passed through the 10-cm cell with $CH_3{}^{15}NH_2$ gas.

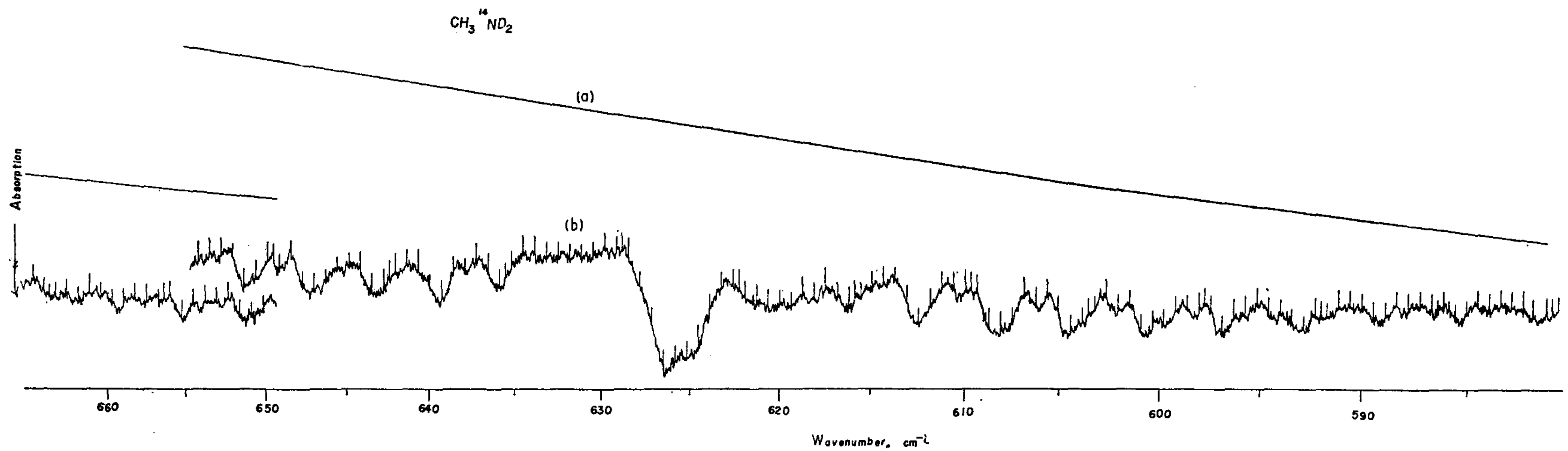

FIG. 4. Infrared absorption spectrum of $CH_3{}^{14}ND_2$ in the 665∼580 cm^{-1} region. (a) Recorded curve for infrared radiation passed through a 10-cm vacuum cell. (b) Recorded curve for infrared radiation passed through the 10-cm cell with $CH_3{}^{14}ND_2$ gas.

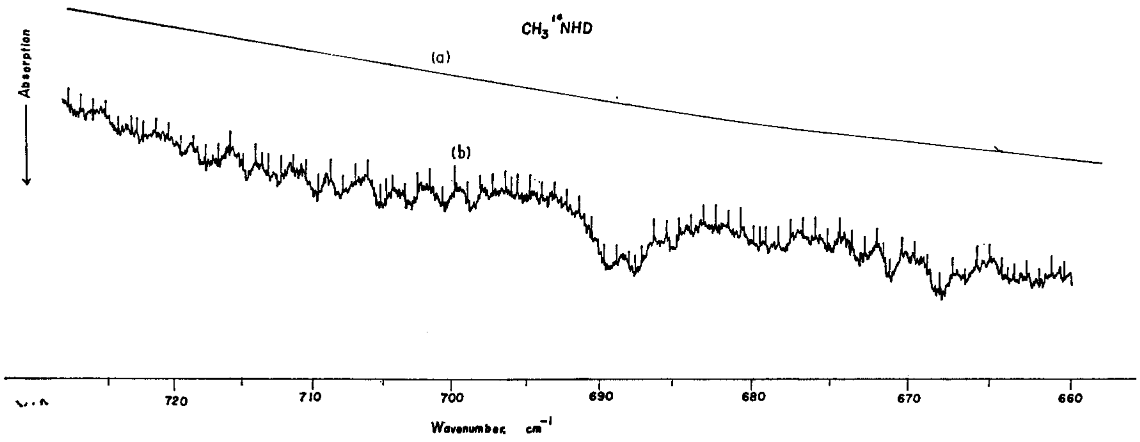

FIG. 5. Infrared absorption spectrum of $CH_3{}^{14}NHD$ in the 730∼660 cm^{-1} region. (a) Recorded curve for infrared radiation passed through a 10-cm vacuum cell. (b) Recorded curve for infrared radiation passed through the 10-cm cell with $CH_3{}^{14}NHD$ gas. In the 680∼660 cm^{-1} region, there is a superposition of the absorptions due to $CH_3{}^{14}ND_2$.

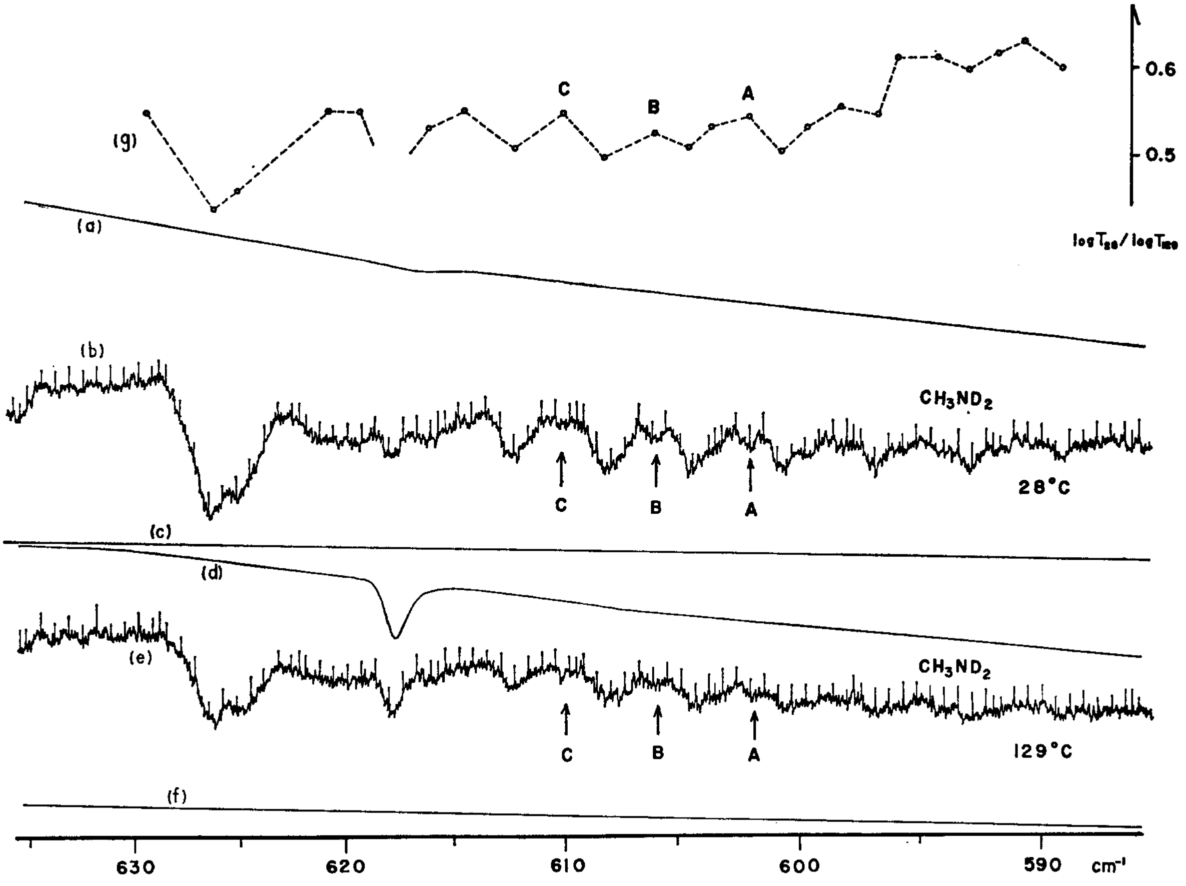

FIG. 6. Infrared absorption spectra of $CH_3{}^{14}ND_2$ observed at different temperatures. (a) and (d): Recorded curves for infrared radiation passed through a 10-cm vacuum cell. (b) and (e): Recorded curves for infrared radiation passed through the 10-cm cell with $CH_3{}^{14}ND_2$ gas. (c) and (f): Recorded curves for no infrared radiation. (g) A plot of the ratio of the absorption intensity (including background absorptions) at 28°C to that at 129°C. T_{28} and T_{129} are the percent transmission/100 at 28° and at 129°C, respectively.

of 1.7 cm^{-1}. In its higher-frequency side there is a series of twin peaks observed. The peak–peak distance within the each pair is about 1.7 cm^{-1}, and the distance from one pair to the adjacent pair is about 4.5 cm^{-1}.

III. THEORETICAL CONSIDERATION

A general theory for the two internal motions (internal rotation and inversion) of the methylamine molecule has been developed by Itoh,[2] and also by Kivelson and Lide,[5] in connection with their analyses of the microwave spectra. The two theories are essentially the same in the basic idea, but the expressions are somewhat different from each other. In analyzing the infrared spectra, we have taken our ground on the same idea, and followed partly the former and partly the latter expressions, with some alterations made by ourselves as given below.

1. Axes and Coordinates

Of the total 21 independent atomic motions of methylamine, five are taken into consideration in this paper. These are the three over-all rotations, internal rotation (x) and wagging-inversion motion (y).

We denote by x the angle of rotation of the methyl group around its symmetry axis with respect to the amino group. The position of $x=0$ is defined as one of the staggered positions.

The wagging-inversion coordinate y is defined as

$$y=2\pi-\beta_1-\beta_2-\gamma. \tag{1}$$

Here, $\beta_1=\angle CNH_4$, $\beta_2=\angle H_5NC$, and $\gamma=\angle H_4NH_5$. (The numbering of the hydrogen atoms in the methylamine molecule is shown in Fig. 1.) It is defined that $y=0$, when the four atoms C, N, H_4, and H_5 come on a plane, that $y>0$ in one side of this position and that $y<0$ in the other side. We defined y in this way rather than in the way of Kivelson and Lide[5] because we found that, in the molecular vibrations of methylamine, a symmetry coordinate $(\Delta\beta_1+\Delta\beta_2+\Delta\gamma)/\sqrt{3}$ is nearer to a normal coordinate than a symmetry coordinate $(\Delta\beta_1+\Delta\beta_2)/\sqrt{2}$ is.

In considering the coupling of the internal rotation and the over-all rotations of the methylamine molecule, we adopt the so-called internal axis method[10]— i.e., we took a system of coordinate axes (ξ, η, ζ) as proposed by Itoh,[2] rather than to use the principal axes (ξ', η', ζ'). Suppose that the amino group of the molecule stays at rest while the methyl group rotates about its own symmetry axis with an angular velocity $\dot{x}$. Let us assume that, in order to give zero resultant angular momentum, the entire molecule need to rotate rigidly with an angular velocity $\boldsymbol{\omega}$. Now a vector $\boldsymbol{\lambda}$ is defined as

$$\boldsymbol{\omega}=\boldsymbol{\lambda}\dot{x}. \tag{2}$$

In the system of coordinate axes (ξ, η, ζ), the ζ axis is directed along the vector $\boldsymbol{\lambda}$. The ξ axis is placed perpendicular to the symmetry plane of the molecule, and the η axis perpendicular to both ξ and ζ axes.

2. Potential Function

Let the azimuthal angles of the N–H_4 and N–H_5 bonds with respect to the C–H_1 bond be ϕ_4 and ϕ_5, respectively (see Fig. 7). Then, the potential energy V_x of the internal rotation may be given in an approximation as

$$V_x=\tfrac{1}{4}H(1+\cos3\phi_4)+\tfrac{1}{4}H(1+\cos3\phi_5). \tag{3}$$

Now, the coordinate x may be defined as

$$x=(\phi_4+\phi_5)/2; \tag{4}$$

we define also that

$$\rho=(\phi_4-\phi_5)/2. \tag{5}$$

By the use of Eqs. (4) and (5), V_x is given as

$$V_x=\tfrac{1}{2}H(1+\cos3\rho\cos3x). \tag{6}$$

In this equation, both H and ρ are functions of the wagging-inversion coordinate y.

H is the height of the potential barrier experienced on rotating from one stable position in the internal rotation to the next stable position. This would be very small if the C, N, H_4, and H_5 atoms were coplanar,[11] while it has a value of 691.1 cm[2,3] when the C, N, H_4, and H_5 atoms are arranged in a pyramidal form as in the equilibrium form ($y=y_0$) of the methylamine molecule. Thus, $H=0$ if $y=0$, and $H=691.1$ cm^{-1} if $y=\pm y_0$. In an approximation, $H(y)$ may be expressed as

$$H=ky^2, \tag{7}$$

where k is a constant.

2ρ is the angle $\angle H_5NH_4$ viewed along the symmetry axis of the methyl group. When $y=y_0$, ρ is nearly $\pi/3$. When $y=0$, ρ is $\pi/2$. When $y=-y_0$, ρ is nearly $2\pi/3$. In these three cases H is given, respectively, by $\tfrac{1}{2}H_0(1-\cos3x)$, 0, and $\tfrac{1}{2}H_0(1+\cos3x)$, where $H_0=ky_0^2=691.1$ cm^{-1}.

The wagging-inversion potential function may be given as

$$V_y=\tfrac{1}{2}ay^2+v\exp(-cy^2), \tag{8}$$

as was chosen by Swalen and Ibers[12] for the inversion of ammonia.

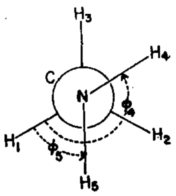

FIG. 7. Azimuthal angles in the internal rotation in the methylamine molecule.

---

[10] C. C. Lin and J. D. Swalen, Rev. Mod. Phys. **31**, 841 (1959).

[11] For CH_3NO_2 and CD_3NO_2, E. Tannenbaum, R. J. Myers, and W. D. Gwinn, J. Chem. Phys. **25**, 42 (1956); For CH_3NO_2, CD_3NO_2, and CH_3BF_2, summarized by D. R. Herschbach, International Symposium on Molecular Structure and Spectroscopy, Tokyo, Paper C401, September 1962.

[12] J. D. Swalen and J. A. Ibers, J. Chem. Phys. **36**, 1914 (1962).

The total potential function is now given as

$$V(x, y)=V_x+V_y. \tag{9}$$

The form of this potential function is schematically illustrated in Fig. 8. In the present analysis given below in this paper, no detailed discussion has been attempted of the form of such a two-dimensional potential function. We suppose, however, that the data of the vibrational excited states of this molecule obtained by the infrared absorption measurements with a higher resolution would enable us to determine the potential forms more precisely in future.

3. Hamiltonian

The complete Hamiltonian for the present problem may be expressed in the form of

$$\mathbf{H}=\mathbf{H}_r+\mathbf{H}_w, \tag{10}$$

where $\mathbf{H}_r$ is the rotational Hamiltonian,

$$\mathbf{H}_r=\tfrac{1}{2}U^{-1}(P_x+\lambda P_\zeta)^2+\tfrac{1}{2}\sum_{\xi,\eta}I^{-1}{}_{\xi\eta}P_\xi P_\eta+V_x, \tag{11}$$

and $\mathbf{H}_w$ is the Hamiltonian for the wagging-inversion motion,

$$\mathbf{H}_w=(1/2\mu)P_y{}^2+V_y. \tag{12}$$

In Eqs. (11) and (12), P_x and P_y are the momenta conjugate, respectively, to x and y. P_ξ, P_η, and P_ζ are the components of the total angular momentum, respectively, along the ξ, η, and ζ axes. $\mathbf{I}$ is the inertia tensor referred to the coordinate axes ξ, η, ζ;

$$U=I_{\mathrm{CH}_3}-\boldsymbol{\lambda}^T\mathbf{I}\boldsymbol{\lambda}, \tag{13}$$

where I_{CH_3} is the moment of inertia of methyl group about its own symmetry axis. λ is the absolute value of $\boldsymbol{\lambda}$, and μ is the reduced mass of the wagging-inversion motion. The superscript ^{T} indicates transpose.

4. Basis Functions

We attempt to obtain approximate eigenvalues of the Hamiltonian (10) by the application of perturbation theory.[5] In order to construct suitable basis functions, let us examine eigenfunctions for some parts of the Hamiltonian (10).

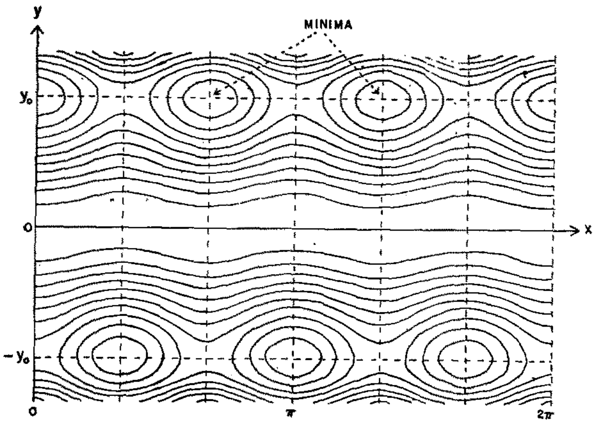

FIG. 8. A schematic drawing of the contour map of the two-dimensional potential function in the internal motions (x and y) of methylamine molecule.

First the Hamiltonian for the internal rotation

$$\mathbf{H}_{\mathrm{i.r.}}=\tfrac{1}{2}U^{-1}(P_x+\lambda P_\zeta)^2+V_x, \tag{14}$$

where

$$V_x=\tfrac{1}{2}H_0(1-\cos 3x), \tag{15}$$

can be solved as has been done by Koehler and Dennison.[13] We denote by $Q(x)$ the eigenfunction of the Hamiltonian (14). Thus we put

$$\tfrac{1}{2}\hbar^2U^{-1}(i^{-1}(d/dx)+\lambda K)^2Q_{K\sigma n}(x)$$
$$+\tfrac{1}{2}H_0(1-\cos 3x)Q_{K\sigma n}(x)=E_{K\sigma n}Q_{K\sigma n}(x). \tag{16}$$

In this equation,

$$K=0, 1, 2, \cdots, \tag{17}$$

is the rotational quantum number so that $K\hbar$ is the eigenvalue of P_ζ;

$$\sigma=0, +1, \quad \text{or} \quad -1 \tag{18}$$

is the internal rotation (i.r.) quantum number (see Sec. IV. 2);

$$n=0, 1, 2, \cdots \tag{19}$$

is the vibrational quantum number of the torsional oscillation along x; and $E_{K\sigma n}$ is the eigenvalue of $\mathbf{H}_{\mathrm{i.r.}}$ now in question.

Secondly, Hamiltonian (12) is to be solved. This would be similar to the Hamiltonian for the umbrella motion of the ammonia molecule.[12,14] The corresponding eigenfunctions can be expressed in terms of an approximate harmonic-oscillator quantum number

$$v=0, 1, 2, \cdots, \tag{20}$$

and for each v there exists an even $[\psi_{v+}(y)]$ and an odd $[\psi_{v-}(y)]$ state. Let us denote by E_{v+} the eigenvalue corresponding to the former and by E_{v-} that corresponding to the latter. As in the case of ammonia, E_{v-} is considered to be higher than E_{v+}.

The eigenvalues for $\frac{1}{2}\sum_{\xi,\eta}I^{-1}{}_{\xi\eta}P_\xi P_\eta$ are to be calculated in a way proper for asymmetric-top molecules. As will be shown later (Sec. IV. 1), however, the methylamine molecule is nearly a symmetric-top molecule and the ξ, η, and ζ axes are directed nearly along the principal axes. Therefore, if we adopt the wavefunctions of a symmetric-top molecule:

$$(1/2\pi)\exp(iK\phi)\exp(iM\psi)\Theta_{J,K,M}(\theta), \tag{21}$$

---

[13] J. S. Koehler and D. M. Dennison, Phys. Rev. **57**, 1006 (1940).

[14] D. M. Dennison and G. E. Uhlenbeck, Phys. Rev. **41**, 313 (1932).

as the basis functions, then the off-diagonal elements of $\frac{1}{2}\sum_{\xi,\eta}I_{\xi\eta}^{-1}P_\xi P_\eta$ are very small.[15] The diagonal element E_{JK} expresses the rotational energy when the molecule is assumed to be a rigid symmetric rotor.

In the methylamine molecule, two protons on the amino group (H_4 and H_5 in Fig. 1) can be exchanged by inversion followed by the 180° rotation of the angle x plus 180° rotation of the angle ϕ. This operation corresponds to a set of transformations of the wavefunctions,

$$\begin{aligned}&(1/\sqrt{2})[\psi_{v+}(y)+\psi_{v-}(y)]\\&\qquad\rightarrow(1/\sqrt{2})[\psi_{v+}(-y)+\psi_{v-}(-y)]\\&\qquad=(1/\sqrt{2})[\psi_{v+}(y)-\psi_{v-}(y)],\\&Q_{K\sigma n}(x)\rightarrow Q_{K\sigma n}(x+\pi),\\&\exp(iK\phi)\rightarrow\exp[iK(\phi+\pi)]=(-1)^K\exp(iK\phi).\end{aligned}\tag{22}$$

Since the Hamiltonian is invariant under this operation, the correct wavefunctions should be either symmetric or antisymmetric with respect to this operation. Therefore, the basis functions are now chosen in the following way:

$$\begin{aligned}\Phi^s{}_{JKM\sigma nv}=&(1/4\pi)\exp(iK\phi)\exp(iM\psi)\Theta_{JKM}(\theta)\\&\times\{(\psi_{v+}+\psi_{v-})Q_{K\sigma n}(x)+(-1)^K(\psi_{v+}-\psi_{v-})Q_{K\sigma n}(x+\pi)\},\end{aligned}\tag{23}$$

$$\begin{aligned}\Phi^a{}_{JKM\sigma nv}=&(1/4\pi)\exp(iK\phi)\exp(iM\psi)\Theta_{JKM}(\theta)\\&\times\{(\psi_{v+}+\psi_{v-})Q_{K\sigma n}(x)-(-1)^K(\psi_{v+}-\psi_{v-})Q_{K\sigma n}(x+\pi)\}.\end{aligned}\tag{24}$$

5. Approximate Solution

For analyzing the present infrared spectra, it has been found to be sufficient to calculate only the diagonal elements of the Hamiltonian (10). These elements are given as

$$\begin{aligned}\int\Phi^{s*}\mathbf{H}\Phi^s dz=&E_{JK}+E_{K\sigma n}\\&+\frac{E_{v+}+E_{v-}}{2}-(-1)^K\left(\frac{E_{v-}-E_{v+}}{2}\right)\\&\times\int_0^{2\pi}Q_{K\sigma n}(x)^*Q_{K\sigma n}(x+\pi)dx\end{aligned}\tag{25}$$

and

$$\begin{aligned}\int\Phi^{a*}\mathbf{H}\Phi^a dz=&E_{JK}+E_{K\sigma n}\\&+\frac{E_{v+}+E_{v-}}{2}+(-1)^K\left(\frac{E_{v-}-E_{v+}}{2}\right)\\&\times\int_0^{2\pi}Q_{K\sigma n}(x)^*Q_{K\sigma n}(x+\pi)dx.\end{aligned}\tag{26}$$

In deriving these expressions of the elements a further approximation,

$$\begin{aligned}&\int_{-\infty}^{+\infty}\psi_{v+}(y)^*V_x(y)\psi_{v+}(y)dy\\&\cong\int_{-\infty}^{+\infty}\psi_{v-}(y)^*V_x(y)\psi_{v-}(y)dy\\&\cong\tfrac{1}{2}H_0(1-\cos 3x),\end{aligned}\tag{27}$$

has been adopted. In a more detailed analysis than that attempted in the present study, this approximation is to be removed and also off-diagonal elements of the Hamiltonian (10) should be taken into account.

IV. NUMERICAL CALCULATIONS

1. Evaluation of the Moments of Inertia, and of λ, U, etc.

To facilitate the numerical calculation, we start with a coordinate system (ξ'', η'', ζ''), where the origin is placed at the center of gravity of the molecule, the ξ'' axis is directed perpendicular to the symmetry plane of the molecule, and the ζ'' axis is directed parallel to the symmetry axis of the methyl group. Let the elements of the inertia tensor $\mathbf{I}''$ be denoted as

$$\mathbf{I}''=\begin{array}{c}\xi''\\\eta''\\\zeta''\end{array}\begin{pmatrix}A&0&0\\0&B&-D\\0&-D&C\end{pmatrix}.\tag{28}$$

The coordinate system (ξ, η, ζ) adopted above in Sec. III. 1, and the system of principal axes (ξ', η', ζ') are related to this (ξ'', η'', ζ'') system as

$$\begin{pmatrix}\xi\\\eta\\\zeta\end{pmatrix}=\begin{pmatrix}1&0&0\\0&\cos\delta&\sin\delta\\0&-\sin\delta&\cos\delta\end{pmatrix}\begin{pmatrix}\xi''\\\eta''\\\zeta''\end{pmatrix}\tag{29}$$

and

$$\begin{pmatrix}\xi'\\\eta'\\\zeta'\end{pmatrix}=\begin{pmatrix}1&0&0\\0&\cos\epsilon&\sin\epsilon\\0&-\sin\epsilon&\cos\epsilon\end{pmatrix}\begin{pmatrix}\xi''\\\eta''\\\zeta''\end{pmatrix},\tag{30}$$

---

[15] In the functions (21), ϕ, ψ, and θ are the Eulerian angles which describe the orientation of the (ξ, η, ζ) axes with respect to a space-fixed axes X, Y, Z. Thus, θ is the angle between the ζ and Z axes, ϕ is the angle between the ξ axis and the line formed by the intersection of the $\xi\eta$ and XY planes; it measures the turning of the molecule about its ζ axis. The angle ψ is the angle between the X axis and the line formed by the intersection of the $\xi\eta$ and XY planes and gives the turning of the whole body about the Z axis. $M=0$, ±1, $\pm2,\cdots$, $\pm J$ is the magnetic quantum number. $\Theta_{J,K,M}(\theta)$ is a known function of θ, and when $K=0$ this is the normalized associated Legendre polynomial of degree J and order $|M|$.

TABLE I. Moments of inertia and other constants in the methylamine and its isotopic molecules, calculated on the assumption that C–H=1.093 Å, N–H=1.014 Å, C–H=1.474 Å, $\alpha(<\mathrm{HCH})=109°30'$, $\beta(<\mathrm{CNH})=112°10'$, $\gamma(<\mathrm{HNH})=105°50'$, and $\chi=3°30'$, where χ is the angle ($\zeta''\rightarrow$C–N bond).

		$CH_3{}^{14}NH_2$	$CH_3{}^{15}NH_2$	$CH_3{}^{14}ND_2$	$CH_3{}^{14}NHD$[a]
A	$(\times 10^{-40}\ \mathrm{g\cdot cm^2})$	37.248	38.085	41.850	39.621
B	$(\times 10^{-40}\ \mathrm{g\cdot cm^2})$	38.891	39.720	45.287	42.121
C	$(\times 10^{-40}\ \mathrm{g\cdot cm^2})$	8.069	8.077	10.649	9.331
D	$(\times 10^{-40}\ \mathrm{g\cdot cm^2})$	−0.204	−0.287	1.083	0.460
d[b]	$(\mathrm{cm^{-1}})$	5.47	5.49	3.96	4.63
$I_{\mathrm{CH_3}}$	$(\times 10^{-40}\ \mathrm{g\cdot cm^2})$	5.333	5.333	5.333	5.333
δ		0°18′	0°25′	−1°22′	···
ϵ		0°23′	0°31′	−1°47′	···
λ		0.6610	0.6604	0.5021	0.5759
U	$(\times 10^{-40}\ \mathrm{g\cdot cm^2})$	1.8079	1.8111	2.6557	2.2642

[a] For $CH_3{}^{14}NHD$, none of the elements of the inertia tensor is zero, and $E=I_{\xi\eta}=0.4636$ and $F=I_{\xi\zeta}=1.5160\times 10^{-40}\mathrm{g\cdot cm^2}$ are to be added to this table. In this molecule, $\boldsymbol{\lambda}$ is not in the $\eta''\zeta''$ plane, and has three nonzero components instead of two. Its absolute value λ is calculated by a formula somewhat different from Eq. (33), while U is calculated by Eq. (13).

[b] $d=(h/4\pi^2c)(C^{-1}-\frac{1}{2}A^{-1}-\frac{1}{2}B^{-1})$. This gives the approximate distance between the adjacent ${}^PQ$ or ${}^RQ$ branch absorptions in a perpendicular band.

where

$$\delta=-\tan^{-1}(D/B) \tag{31}$$

and

$$\epsilon=-\tfrac{1}{2}\tan^{-1}[2D/(B-C)] \tag{32}$$

are the angles ($\zeta''\rightarrow\zeta$) and ($\zeta''\rightarrow\zeta'$), respectively. The positive direction of these angles is defined as that of the counterclockwise rotation viewed along the line perpendicular to the symmetry plane with the amino group placed upward on the right side of the C–N bond (as in Fig. 1). As is shown by Itoh,[2] λ and U are given by

$$\lambda=I_{\mathrm{CH_3}}(B^2+D^2)^{\frac{1}{2}}/(BC-D^2) \tag{33}$$

and

$$U=I_{\mathrm{CH_3}}[B(C-I_{\mathrm{CH_3}})-D^2]/(BC-D^2). \tag{34}$$

In Table I are given the values of A, B, C, D, $I_{\mathrm{CH_3}}$, δ, ϵ, λ, and U calculated by the use of the molecular parameters given by Itoh[2] and Nishikawa.[3]

2. Eigenvalues of the Internal Rotation

To solve Eq. (16), let $Q_{K\sigma n}(x)$ be expanded in the Fourier series

$$Q_{K\sigma n}(x)=\sum_{m=-\infty}^{+\infty} a_m \exp(imx), \tag{35}$$

where m is an integer. Substituting (35) into Eq. (16), we obtain the relation

$$\begin{aligned}\mathbf{H}_{\mathrm{i.r.}}Q(x)&=\sum_m[\tfrac{1}{2}\hbar^2U^{-1}(m+\lambda K)^2+\tfrac{1}{2}H_0]a_m\exp(imx)\\&\quad-\sum_m\tfrac{1}{4}H_0a_{m-3}\exp(imx)-\sum_m\tfrac{1}{4}H_0a_{m+3}\exp(imx)\\&=E_{K\sigma n}\sum_m a_m\exp(imx).\end{aligned} \tag{36}$$

The matrix expression of this equation can be factored into three as written below;

$$\begin{pmatrix}\ddots & & & \\ & \frac{1}{2}\hbar^2U^{-1}(3+\sigma+\lambda K)^2+\frac{1}{2}H_0 & -\frac{1}{4}H_0 & 0 & \\ & -\frac{1}{4}H_0 & \frac{1}{2}\hbar^2U^{-1}(0+\sigma+\lambda K)^2+\frac{1}{2}H_0 & -\frac{1}{4}H_0 & \\ & 0 & -\frac{1}{4}H_0 & \frac{1}{2}\hbar^2U^{-1}(-3+\sigma+\lambda K)^2+\frac{1}{2}H_0 & \\ & & & & \ddots\end{pmatrix}\begin{pmatrix}\vdots\\ a_{3+\sigma}\\ a_{0+\sigma}\\ a_{-3+\sigma}\\ \vdots\end{pmatrix}=\mathbf{E}_\sigma\begin{pmatrix}\vdots\\ a_{3+\sigma}\\ a_{0+\sigma}\\ a_{-3+\sigma}\\ \vdots\end{pmatrix}, \tag{37}$$

where $\sigma=0$, $+1$, or -1 (see Sec. III. 4). $\mathbf{E}_\sigma$ is the diagonal matrix where all the diagonal elements are $E_{K\sigma n}$. Inspection of Eq. (37) shows that $E_{K\sigma n}$ for a given $\sigma+\lambda K$ takes an equal value to that for $\sigma+\lambda K+3$. Therefore, $E_{K\sigma n}$ should be a periodic function of

$$\Omega=\tfrac{2}{3}\pi(\sigma+\lambda K), \tag{38}$$

that is,

$$E_{K\sigma n}=e_n+e_n'\cos\Omega+e_n''\cos 2\Omega+\cdots. \tag{39}$$

As has been pointed out by Lin and Swalen,[10] the solutions of a Mathieu equation of the type of Eq. (16) are in general nonperiodic. However, if $\sigma=0$ and $\lambda K=0$, the solutions are of period π, and the corresponding

TABLE II. Eigenvalues $E_{K\sigma n}$ of the torsional equation (16), and overlap integral $G_{K\sigma n}$. The barrier height H_0 is assumed to be 691.1 cm^{-1}.

	$CH_3{}^{14}NH_2$	$CH_3{}^{15}NH_2$	$CH_3{}^{14}ND_2$	$CH_3{}^{14}NHD$
s^a	19.832	19.867	29.132	24.837
E_{000}(cm^{-1})	145.70	145.56	121.76	131.23
E_{010}(cm^{-1})	145.95	145.83	121.80	131.32
e_0 (cm^{-1})	145.86	145.74	121.79	131.29
e_0' (cm^{-1})	−0.17	−0.18	−0.03	−0.06
G_{000}	0.2153	0.2148	0.1226	0.1568
G_{010}	−0.1083	−0.1080	−0.0614	−0.0786
g_0'	0.2157	0.2152	0.1226	0.1570
g_0'''	−0.0004	−0.0004	-0.0000_6	-0.0001_2

[a] s is the coefficient of $\cos^2 x$ in the standard form Mathieu equation of which eigenvalues and eigenfunctions are tabulated.[16,17] It is shown that the values of s can be determined by the relation $s=8UH_0/9\hbar^2$.

eigenvalues can be found from Ref. 16. The lowest eigenvalue (for $n=0$), thus found, is given in Table II. If $\sigma=1$ and $\lambda K=0$, the solutions are of period 3π. The eigenvalues in this case can be found in other tables given by Kilb.[17] The result for $n=0$ is given in Table II. In finding these eigenvalues, the barrier height H_0 in the internal rotation potential was assumed to be 691.1 cm^{-1}.[2,3] Since $E(\lambda K=0,\ \sigma=1,\ n=0,)=E(\lambda K=1,\ \sigma=0,\ n=0)$, we obtain for $CH_3{}^{14}NH_2$,

$$E_{K,0,0}=145.86-0.17\cos\tfrac{2}{3}\pi\lambda K,$$

$$E_{K,+1,0}=145.86-0.17\cos\tfrac{2}{3}\pi(\lambda K+1), \tag{40}$$

and

$$E_{K,-1,0}=145.86-0.17\cos\tfrac{2}{3}\pi(\lambda K-1)$$

in reciprocal centimeters, assuming that $e_0''=0$.

3. Evaluation of the Overlap Integral $G_{K\sigma n}$ [Eq. (43)]

From Eqs. (25) and (26), the inversion splitting Δ of an energy level with a set of quantum numbers K, σ, n, and v is expressed as

$$\Delta=(-1)^K\Delta_v\int_0^{2\pi}Q_{K\sigma n}(x)^*Q_{K\sigma n}(x+\pi)dx. \tag{41}$$

Here, the sign is defined to be positive when the antisymmetric (with respect to the proton exchange operation given in III.4) level is higher than the symmetric level. Thus, Δ_v means

$$\Delta_v=E_{v-}-E_{v+}. \tag{42}$$

Now we need to evaluate the overlap integral

$$G_{K\sigma n}=\int_0^{2\pi}Q_{K\sigma n}(x)^*Q_{K\sigma n}(x+\pi)dx \tag{43}$$

and to examine how it depends upon K and σ. An inspection of Eq. (37) shows that

$$a_m(\lambda K+3)=a_{m+3}(\lambda K). \tag{44}$$

This leads to a relation

$$Q(\lambda K+3,x)=Q(\lambda K,x)\exp(-i3x). \tag{45}$$

Therefore,

$$\int_0^{2\pi}Q(\lambda K+3,x)^*Q(\lambda K+3,x+\pi)dx$$

$$=-\int_0^{2\pi}Q(\lambda K,x)^*Q(\lambda K,x+\pi)dx. \tag{46}$$

From this relation, it is concluded that the overlap integral $G_{K\sigma n}$, now in question, should be a periodic function of $\frac{1}{3}\pi\lambda K$ and should be expanded in a Fourier series in which only odd multiples of $\frac{1}{3}\pi\lambda K$ appear. It is also seen in Eq. (37) that

$$a_\sigma(\lambda K+1)=a_{\sigma+1}(\lambda K).^{18} \tag{47}$$

Therefore,

$$Q_\sigma(\lambda K+1,x)=Q_{\sigma+1}(\lambda K,x)\exp(-ix), \tag{48}$$

or

$$\int_0^{2\pi}Q_\sigma(\lambda K+1,x)^*Q_\sigma(\lambda K+1,x+\pi)dx$$

$$=-\int_0^{2\pi}Q_{\sigma+1}(\lambda K,x)^*Q_{\sigma+1}(\lambda K,x+\pi)dx. \tag{49}$$

Combining Eqs. (46) and (49), we obtain

$$\int_0^{2\pi}Q_\sigma(\lambda K+4,x)^*Q_\sigma(\lambda K+4,x+\pi)dx$$

$$=-\int_0^{2\pi}Q_\sigma(\lambda K+1,x)^*Q_\sigma(\lambda K+1,x+\pi)dx$$

$$=\int_0^{2\pi}Q_{\sigma+1}(\lambda K,x)^*Q_{\sigma+1}(\lambda K,x+\pi)dx. \tag{50}$$

---

[16] *Tables Relating to Mathieu Functions* (Columbia University Press, New York, 1951).

[17] R. W. Kilb, *Tables of Mathieu Eigenvalues and Eigenfunctions for Special Boundary Conditions* (Department of Chemistry, Harvard University, 1956). We are grateful to E. Hirota for his lending us a copy of these tables.

[18] Here, it is defined that $\sigma+1=-1$ if $\sigma=+1$.

This means that if σ increases by 1 and λK decreases by 4, the overlap integral in question remains unchanged. Therefore, it may be concluded[2] that

$$G_{K\sigma n}=g_n'\cos[\tfrac{1}{3}\pi\lambda K+\tfrac{4}{3}\pi\sigma]+g_n'''\cos 3[\tfrac{1}{3}\pi\lambda K+\tfrac{4}{3}\pi\sigma]+\cdots. \qquad (51)$$

On the other hand, if we know the values of the a_m's [see Eq. (35)] for a set of K, σ, and n, the corresponding $G_{K\sigma n}$ value is calculated by the formula

$$G_{K\sigma n}=2\pi N\sum_{m=-\infty}^{\infty}a_m^2\exp(im\pi), \qquad (52)$$

where the normalization factor N can be obtained by the relation

$$\frac{1}{N}=2\pi\sum_{m=-\infty}^{\infty}a_m^2. \qquad (53)$$

In special cases where $K=0$, the values of a_m's can be found in the tables[16,17] cited above. From these values of the a_m's, the overlap integral G_{000} and G_{010} are calculated. The results are given in Table II. By the use of these values, and also by the use of the relations

$$G(\lambda K=0,\sigma=1,n=0)=G(\lambda K=4,\sigma=0,n=0), \quad \text{etc.,}$$

we obtain for $CH_3{}^{14}NH_2$:

$$G_{K,0,0}=0.2157\cos\tfrac{1}{3}\pi\lambda K-0.0004\cos\pi\lambda K,$$

$$G_{K,+1,0}=0.2157\cos\tfrac{1}{3}\pi(\lambda K+4)-0.0004\cos\pi(\lambda K+4),$$

$$G_{K,-1,0}=0.2157\cos\tfrac{1}{3}\pi(\lambda K-4)-0.0004\cos\pi(\lambda K-4). \qquad (54)$$

V. ANALYSIS OF THE SPECTRA

1. $CH_3{}^{14}NH_2$

The general scheme of the splittings of the energy levels is illustrated in Fig. 9. We are dealing with a transition from one of the rotational levels ($K=K''$) in the vibrational ground state ($v_{\text{wag}}=0$) to a vibration–rotation level with $v_{\text{wag}}=1$ and $K=K'$. Each of these two levels split into three sublevels with $\sigma=0$, $+1$, and -1 because of the internal rotation. This splitting is very small [0.2 cm^{-1} or so; see Eq. (40)] at $n=0$. However, each of these sublevels splits widely into two due to the inversion. One of these component levels of the inversion doublet is symmetric and the other is antisymmetric with respect to the exchange of the positions of two protons in the NH_2 group. The nuclear statistical weights of these levels are 1 and 3, respectively. Thus, each of the vibration–rotation levels splits into six levels due to the internal motions. Selection rules are $\Delta\sigma=0$, singlet↔singlet, and triplet↔triplet. Therefore, six transitions with different frequencies should be observed instead of the usual one $K''\rightarrow K'$ transition.

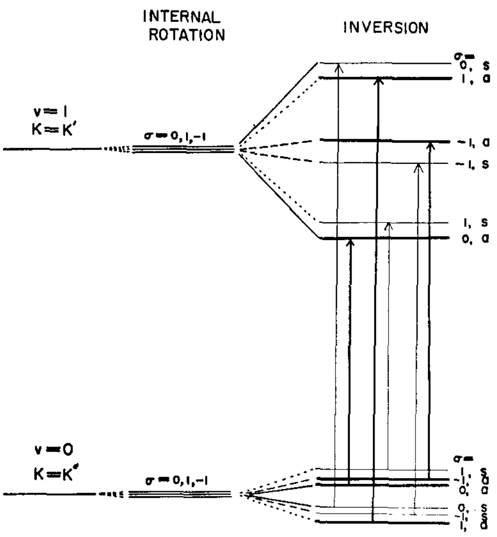

FIG. 9. Schematic illustration of the splittings of the vibration–rotation levels due to the internal motions of the methylamine molecule and transitions between these levels. The thick horizontal lines show triplet levels and the thin lines singlet levels of CH_3NH_2.

We are now to draw a theoretical spectrum on the basis of what has been described. The transition moment of the amino-wagging band in question is considered to be oriented obliquely to both of the ζ and η axes, and therefore we may expect both the parallel and perpendicular components in the fine structure of this band. If there were no internal motions coupling with the rotation of the molecule, we would expect, at the band center, a strong absorption peak (^QQ branch) of the parallel component corresponding to the transitions with $\Delta J=0$ and $\Delta K=0$. Actually, we observe a plateau with a complicated structure and of about 7–8 cm^{-1} in width in the vicinity of the band center. This fact may be interpreted as due to the splitting of each of the component lines in the ^QQ branch. The width W of this plateau may roughly be related to the already introduced quantities (g_0', Δ_0, and Δ_1) as

$$W=g_0'(\Delta_1-\Delta_0). \qquad (55)$$

For $CH_3{}^{14}NH_2$, we know that $g_0'=0.2157$ and $\Delta_0=0.9535$ cm^{-1}.[2,3] Hence, Δ_1 is estimated to be 32–36 cm^{-1}. After a few trials, we have reached a conclusion that the observed spectrum is most satisfactorily explained on the assumption that $\Delta_1=31.6$ cm^{-1}.

In Fig. 10, a comparison is made of the calculated and observed spectra. At the top of this figure expected perpendicular component is shown. The band center was assumed to be placed at 780.1 cm. The vertical

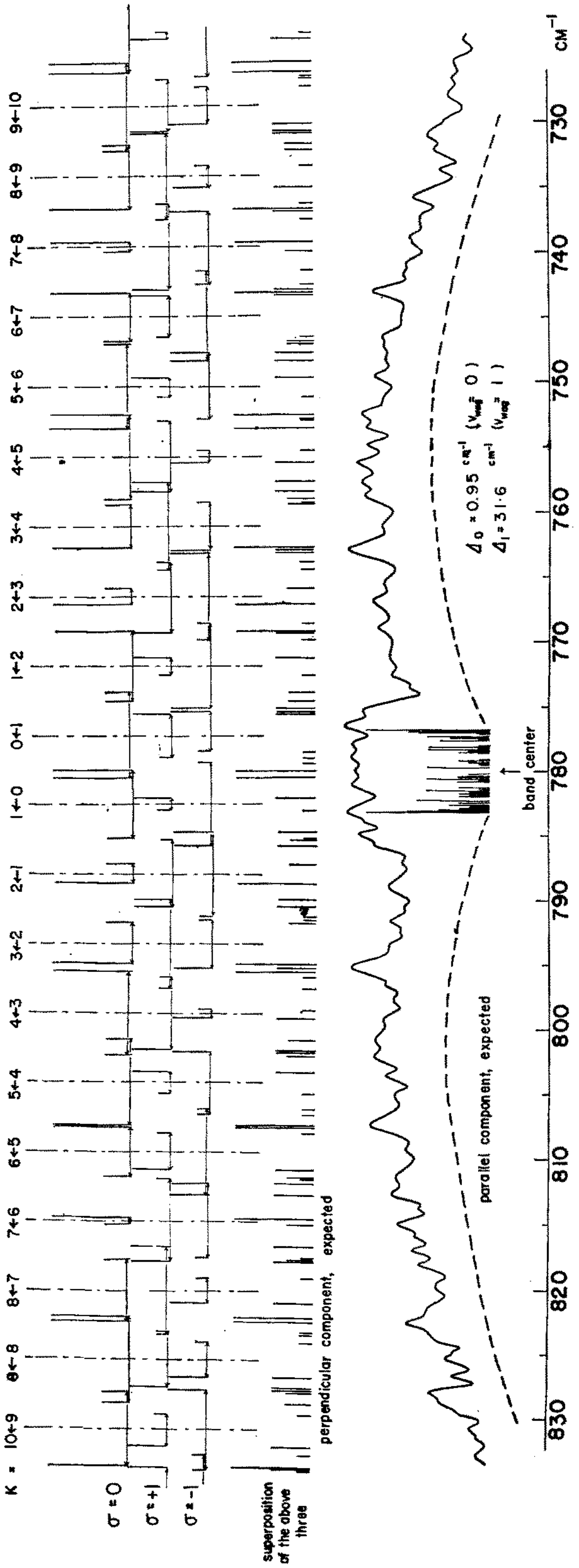

FIG. 10. A comparison of the calculated and observed infrared absorption spectra of $CH_3{}^{14}NH_2$ in the 835~725 cm^{-1} region.

—•—• lines indicate the hypothetical positions of the $^PQ(\Delta J=0,\ \Delta K=-1)$ and $^RQ(\Delta J=0,\ \Delta K=1)$ branch absorptions which would be expected when the internal motions were absent. These lines are placed with an equal spacing of

$$\frac{h}{4\pi^2 c}[C^{-1}-\tfrac{1}{2}A^{-1}-\tfrac{1}{2}B^{-1}]=5.4\ \mathrm{cm}^{-1},$$

where c is the light velocity and $A=37.248\times10^{-40}$, $B=38.891\times10^{-40}$, and $C=8.069\times10^{-40}$ g·cm² (see Table I). A slight shifting which is to be expected for each of these positions because of the asymmetry of the molecule and also because of the nonrigidity of the molecule has been neglected. The splitting of these hypothetical absorptions due to the internal rotation can be calculated by the use of Eq. (40). However, we have neglected this splitting, too, for a while, because it is very small [less than 0.2 cm^{-1}, see Eq. (40)] and it does not cause much difference in the calculated spectrum to be compared with the infrared spectrum observed with relatively poor resolution such as what we are now dealing with. Each of the hypothetical ^PQ and ^RQ branch absorptions is expected to split into six peaks. The width of the splitting has been calculated on the basis of Eq. (54), and the expected positions of the absorption peaks are shown in the figure. Here, a singlet→singlet transition and a triplet→triplet transition are distinguished with different lengths (1:3) of the vertical lines. Also every line with $\sigma=0$ is made twice as long as the corresponding line with $\sigma=1$ or $\sigma=-1$, because of the spins of the protons on the methyl group. On drawing the calculated spectrum of the parallel component (given at the bottom of Fig. 10), we divided the central plateau region into subregions with 0.10 cm^{-1} in width. All the absorption lines expected to fall in each subregion were added in a head-to-tail way so that only one long line is assigned to each subregion. Here again, Length 3 was assigned to each triplet→triplet transition and Length 1 to the corresponding singlet→singlet transition. In addition, every line with $\sigma=0$ was made twice as long as the corresponding line with $\sigma=1$ or -1. The P and R branch absorptions ($\Delta J=\pm1$) in both of the parallel and perpendicular components are considered to contribute only as background absorptions, and therefore are not taken into account in predicting the fine structure of the band. The observed spectrum is reproduced as a continuous curve in Fig. 10. As may be seen, most of the strong absorption peaks and many of the weak absorption peaks observed are well correlated to the predicted absorption lines.

On the basis of the result of this comparison, we may draw the following two conclusions with certainty: (1) At least in a first approximation, the inversion splitting can be given by Eq. (41), not only for $v_{\mathrm{wag}}=0$[2,3] but also for $v_{\mathrm{wag}}=1$. (2) The hypothetical inversion splitting when the coupling between the inversion and internal rotation were absent is 31.6 cm^{-1} for the first excited state of the amino-wagging vibration of $CH_3{}^{14}NH_2$.

From the latter conclusion, we may predict that the inversion potential feature in methylamine is similar to that of ammonia. We would like to postpone a more detailed discussion on the potential, however, until we obtain more precise data of the inversion splitting in $CH_3{}^{14}ND_2$ than we do in this investigation (see below).

2. $CH_3{}^{15}NH_2$

As may be seen in Tables I and II, the values of constants d, λ, e_0', g_0', and g_0''' of $CH_3{}^{15}NH_2$ are all expected to be very close to the corresponding values of $CH_3{}^{14}NH_2$. On the other hand, one might expect an appreciable difference in the Δ_1 value, because the reduced mass in the wagging-inversion motion along y in Eq. (1) of $CH_3{}^{15}NH_2$ should be about 0.7% higher than that of $CH_3{}^{14}NH_2$. In the case of the symmetric deformation motion in the ammonia molecule, the reduced mass of ${}^{15}NH_3$ is considered to be 1.0% higher than that of ${}^{14}NH_3$, while Δ_1 of ${}^{15}NH_3$ is found[19] to be about 5% lower than Δ_1 of ${}^{14}NH_3$. In the present case, however, we could not detect the difference in Δ_1 from our experimental results given in Figs. 2 and 3.

3. $CH_3{}^{14}ND_2$

If this molecule were rigid, a strong absorption peak (${}^QQ$ branch) at the band center and a series of absorption peaks with a spacing of about 4.0 cm^{-1} (${}^PQ$ and ${}^RQ$ branches) in both sides of the band center would be expected in the fine structure of a hybrid band. Almost at the expected positions, absorption peaks are actually observed (see Fig. 4), with the band center at 625.7 cm^{-1}. Each of these, however, is broad and seems to be a bundle of several unresolved absorption lines. On the basis of the above theory each of these bundles is considered to involve six absorption peaks. Three of them should correspond to transitions from symmetric (with respect to the exchange of the two deuterons in the ND_2 group) levels to symmetric levels and the other three to transitions from antisymmetric levels to antisymmetric levels. The former transitions have twice the statistical weight of the latter. The expected positions of these six absorption peaks can be calculated by the use of Eq. (41) with trial values of Δ_0 and Δ_1. Unfortunately, however, the spectral resolution is not sufficient for comparison of the observed and expected positions of the absorption peaks. Therefore, only a rough estimation of the Δ_1 value has been attempted. From the observed shape of the central ${}^QQ$ branch absorptions, it may be concluded that the maximum inversion splitting is about 1.2 cm^{-1}. Using Eq. (55), and knowing that $g_0'=0.1226$ (see Table II) and that $\Delta_0 \ll 0.95$ cm^{-1}, we are led to a conclusion that the hypothetical pure inversion splitting Δ_1 is of the order of 10 cm^{-1} for the first excited state of ND_2 wagging vibration of $CH_3{}^{14}ND_2$.

One of the ${}^RQ$ branch absorption peaks expected at about 632 cm^{-1}($K=1\rightarrow2$) is not actually observed (see Fig. 4). This fact is attributable to the asymmetry of the $CH_3{}^{14}ND_2$ molecule. For a slightly asymmetric top molecule in general there should be a pair of rotational levels corresponding to the each rotational level (with $K\neq0$) of the limiting symmetric-top molecule. The splitting of the pair of levels is greater for lower K and higher J. In the case of $CH_3{}^{14}ND_2$, it is shown by the use of the moments of inertia given in Table I that the splitting is appreciable for levels with $K=1$. For example, the splitting is about 0.7 cm^{-1}, for the level of $K=1$, $J=5$; it is about 1.0 cm^{-1} for $K=1$, $J=6$. Therefore, it is understandable that the ${}^RQ$ branch absorptions with $K=1\rightarrow2$ and $J=0, 1, 2, \cdots$ do not concentrate at a position and do not give a strong peak.

As has been stated in Sec. II, relatively weak absorption peaks at 602, 606, and 610 cm^{-1} (indicated by A, B, and C in Fig. 6) become stronger on elevating the temperature of $CH_3{}^{14}ND_2$ gas, and, therefore, these peaks are assignable to what belongs to a hot band. We have observed[20] that deuterated methylamine shows a strong absorption band at about 230 cm^{-1} assignable to the C–N torsional vibration ($n=0\rightarrow1$). It is very probable that the hot band expressed as ($n=1$, $v=0$)$\rightarrow$($n=1$, $v=1$) is superposed on the fundamental band ($n=0$, $v=0$)$\rightarrow$($n=0$, $v=1$) now in question. The ratio of the Boltzmann factor corresponding to the energy difference of 230 cm^{-1} is about 1/3.0 at 28°C, while it is about 1/2.3 at 129°C. The observed intensity ratio of the hot-band absorptions to the corresponding fundamental absorptions is in accord with what is expected from the ratio of the Boltzmann factor. The band center of the hot band is probably at 620.5 cm^{-1}.

4. $CH_3{}^{14}NHD$

At the band center of the wagging band of this molecule, there are two strong absorption peaks at 687.7 and 689.4 cm^{-1}. These two are considered to be the ${}^QQ$-branch absorption doubled due to the inversion, with a separation of 1.7 cm^{-1}. In the low-frequency side there is a superposition of the wagging band of $CH_3{}^{14}ND_2$, and this causes an ambiguity. In the high-frequency side, on the other hand, a series of the ${}^RQ$ branch absorption peaks is observed with a spacing of 4.5 cm^{-1}, which is nearly equal to the expected spacing

---

[19] M. Tsuboi (to be published). The data obtained by H. W. Morgan, P. A. Staats, and J. H. Goldstein, J. Chem. Phys. **27**, 1212 (1957) does not seem to be sufficiently accurate.

[20] M. Tsuboi, A. Y. Hirakawa, and K. Tamagake (to be published).

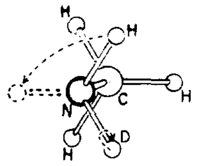

FIG. 11. A probable wagging-inversion coordinate in CH_3NHD.

(see Table I). Each of these absorption peaks seems to be again doubled with the separation of 1.7 cm^{-1}. Thus, what we see in both of the ^{Q}Q- and ^{R}Q-branch absorptions seems to be a typical inversion doubling, and there seems to be no coupling between the inversion and the internal rotation. Our tentative interpretation of this fact is as follows.

In the $CH_3{}^{14}NHD$ molecule, the normal coordinate of the 688.5 cm^{-1} band is greatly different from that of the 780.1-cm^{-1} band in $CH_3{}^{14}NH_2$ or from that of the 625.7-cm^{-1} band of $CH_3{}^{14}ND_2$. In the motion along this coordinate, the N–D bond moves almost in the CND plane, first going up and then going down. The N–H bond moves along an arc and goes directly from minimum to minimum of the torsional potential (see Fig. 11). During this movement, the angles of β_1, β_2, and γ are considered to be kept equal to one another, because this seems to be an essential requirement for keeping the motion nearly along the normal coordinate. The inversion along this coordinate may not couple with the internal rotation, but probably encounters a relatively thick potential barrier. This explains the simple and relatively small inversion doubling observed. The inversion converts one form of the molecule into its mirror image. The statistical weight of the energy level symmetric with respect to this conversion is exactly equal to that of the antisymmetric level. Therefore, the intensities of the component absorption peaks of the each doublet should be equal, as are actually observed.

ACKNOWLEDGMENTS

We wish to express our sincere thanks to Professor T. Shimanouchi and his collaborators for their kindness in allowing us to use a Perkin–Elmer 112 G infrared spectrometer, and for their kind interest in this work. Our thanks are also due to Professor T. Nishikawa and Professor Y. Morino and his collaborators for their valuable discussions. We would also like to thank Mr. A. Nakamura for his providing the sample of ^{15}N-methylamine hydrochloride. This work was supported partly by a grant from the U. S. Public Health Service No. GM 10024-01 and partly by a grant from the Ministry of Education of Japan.